Development 133, 4957-4968 (2006) doi:10.1242/dev.02677

Juxtaposed Polycomb complexes co-regulate vertebral identity

Se Young Kim[1], Suzanne W. Paylor[1], Terry Magnuson[2] and Armin Schumacher[1,*]

Best known as epigenetic repressors of developmental Hox gene transcription, Polycomb complexes alter chromatin structure by means of post-translational modification of histone tails. Depending on the cellular context, Polycomb complexes of diverse composition and function exhibit cooperative interaction or hierarchical interdependency at target loci. The present study interrogated the genetic, biochemical and molecular interaction of BMI1 and EED, pivotal constituents of heterologous Polycomb complexes, in the regulation of vertebral identity during mouse development. Despite a significant overlap in dosage-sensitive homeotic phenotypes and co-repression of a similar set of Hox genes, genetic analysis implicated *eed* and *Bmi1* in parallel pathways, which converge at the level of Hox gene regulation. Whereas EED and BMI1 formed separate biochemical entities with EzH2 and Ring1B, respectively, in mid-gestation embryos, YY1 engaged in both Polycomb complexes. Strikingly, methylated lysine 27 of histone H3 (H3-K27), a mediator of Polycomb complex recruitment to target genes, stably associated with the EED complex during the maintenance phase of Hox gene repression. Juxtaposed EED and BMI1 complexes, along with YY1 and methylated H3-K27, were detected in upstream regulatory regions of *Hoxc8* and *Hoxa5*. The combined data suggest a model wherein epigenetic and genetic elements cooperatively recruit and retain juxtaposed Polycomb complexes in mammalian Hox gene clusters toward co-regulation of vertebral identity.

KEY WORDS: Polycomb, *eed, Bmi1*, Hox genes, Mouse development, Chromatin, Histones, Epigenetics

INTRODUCTION

Originally discovered in *Drosophila*, Polycomb (PcG) proteins are required for epigenetic repression of Hox gene transcription during metazoan development (Francis and Kingston, 2001; Ringrose and Paro, 2004). In mouse embryos, defects in *PcG* function cause de-repression of Hox gene transcription in individual somites anterior to the wild-type Hox expression boundary (van der Lugt et al., 1994; Akasaka et al., 1996; Schumacher et al., 1996; van der Lugt et al., 1996; Coré et al., 1997; Takihara et al., 1997; Katoh-Fukui et al., 1998; del Mar Lorente et al., 2000; Suzuki et al., 2002; Voncken et al., 2003; Isono et al., 2005). This alters the identity of the affected anterior somites toward a more posterior fate and manifests as posterior homeotic transformation of the corresponding vertebrae.

At least two PcG complexes with diverse composition and function in chromatin remodeling have been identified in mammals (Otte and Kwaks, 2003). The Polycomb repressive complex 1 (PRC1) involves the paralogous PcG proteins BMI1/MEL18 (PCGF2 – Mouse Genome Informatics), M33 (CBX2 – Mouse Genome Informatics)/PC2 (PCSK2 – Mouse Genome Informatics)/PC3 (PCSK1 – Mouse Genome Informatics), RAE28 (PHC1 – Mouse Genome Informatics)/MPH2, and RING1A (RING1 – Mouse Genome Informatics)/RING1B (RNF2 – Mouse Genome Informatics) (Alkema et al., 1997a; Alkema et al., 1997b; Gunster et al., 1997; Satijn et al., 1997; Schoorlemmer et al., 1997; Hashimoto et al., 1998; Hemenway et al., 1998; Satijn and Otte, 1999; Levine et al., 2002; Suzuki et al., 2002). Evidence for PRC1-mediated chromatin modification derived from ubiquitylation at lysine 119 of histone H2A (H2A-K119) (de Napoles et al., 2004; Wang, H. et al., 2004; Cao et al., 2005). A second PcG complex, PRC2, encompasses EED, the histone methyltransferase EZH2, the zinc finger protein SUZ12, the histone-binding proteins RBAP46/RBAP48, and the histone deacetylase HDAC1 (Denisenko et al., 1998; Sewalt et al., 1998; van Lohuizen et al., 1998; van der Vlag and Otte, 1999; Cao et al., 2002; Kuzmichev et al., 2002; Kuzmichev et al., 2004). Several EED isoforms, generated by alternate translation start site usage of *eed* mRNA, differentially engage in PRC2-related complexes (PRC2/3/4), targeting the histone methyltransferase activity of EZH2 to H3-K27 or H1-K26 (Kuzmichev et al., 2002; Kuzmichev et al., 2004; Kuzmichev et al., 2005). PcG complexes bind to *cis*-acting Polycomb response elements (PREs), which encompass several hundred base pairs and are necessary and sufficient for PcG-mediated repression of target genes (Pirrotta et al., 2003). Whereas the function of several PREs has been delineated in *Drosophila*, similar elements await characterization in mammals.

Studies in *Drosophila* revealed strong genetic interaction in many, but not all, pairwise combinations of *PcG* mutant alleles (Jürgens, 1985; Kennison and Tamkun, 1988; Adler et al., 1989; Adler et al., 1991; Paro and Hogness, 1991; Cheng et al., 1994; Campbell et al., 1995; Bajusz et al., 2001). For example, Psc and Pc engage in *Drosophila* PRC1 (Shao et al., 1999), and intercrosses between mutant alleles significantly enhanced the homeotic phenotypes compared with the single mutants (Campbell et al., 1995). Likewise, synergistic interaction between mutant alleles of their murine homologs, *Bmi1* and *M33*, was evident from ectopic Hox gene expression and posterior homeotic transformations across multiple adjacent somites and vertebrae, respectively (Bel et al., 1998).

Molecular support for cooperative interaction between PcG complexes derived from the transient association of the ESC/EZ/PHO complex and PRC1 in preblastoderm embryos (Poux et al., 2001). Furthermore, EZH2, in a complex with Esc, methylated histone H3-K27 in the vicinity of PREs, resulting in Pc binding to this epigenetic mark and repression of Hox genes (Cao et al., 2002;

[1]Department of Molecular and Human Genetics, Baylor College of Medicine, Houston, Texas 77030, USA. [2]Department of Genetics, University of North Carolina, Chapel Hill, North Carolina 27599, USA.

*Author for correspondence (e-mail: armins@bcm.tmc.edu)

Accepted 3 October 2006

Czermin et al., 2002; Müller et al., 2002; Wang, L. et al., 2004). In conjunction with similar findings in mammalian cell lines and embryonic stem cells (Kuzmichev et al., 2002; Cao et al., 2005; Fujimura et al., 2006), these results supported a model of hierarchical recruitment of PRC1 to target genes upon binding to PRC2/3/4-methylated H3-K27. Although mammalian cell lines exhibited co-localization of BMI1 with components of PRC2/3/4 in a cell-cycle dependent manner (Hernandez-Munoz et al., 2005), transient interaction between the core PcG complexes has not been reported at the molecular level. Thus, the functional relationship between PRC1 and PRC2/3/4 in the regulation of vertebral identity remains elusive.

The present study interrogated the genetic and molecular interplay of BMI1 and EED, pivotal constituents of PRC1 and PRC2/3/4, respectively, in axial Hox gene repression in the mouse embryo. *Bmi1* (B cell-specific Mo-MLV integration site 1) encodes a 324 amino acid ring finger protein, which interacts directly with RAE28, RING1A, RING1B and M33 (Alkema et al., 1997a; Gunster et al., 1997; Satijn et al., 1997). In conjunction with RING1A, BMI1 is required for ubiquitylation of H2A-K119 (de Napoles et al., 2004; Wang, H. et al., 2004; Cao et al., 2005). A loss-of-function allele of *Bmi1* demonstrated ectopic Hox gene expression and highly penetrant, dosage-sensitive posterior homeotic transformations along the vertebral column (van der Lugt et al., 1994; van der Lugt et al., 1996). *Bmi1*-deficient mice died between birth and 20 weeks of age and displayed neurological and hematopoietic abnormalities (van der Lugt et al., 1994; Lessard et al., 1999).

eed (embryonic ectoderm development) encodes a 535 amino acid protein with five WD motifs and is likely to adopt a toroidal β-propeller structure (Schumacher et al., 1996; Denisenko and Bomsztyk, 1997; Ng et al., 1997; Schumacher et al., 1998; Sewalt et al., 1998; Kuzmichev et al., 2004). Integrity of the WD motifs is essential for protein interaction, and two point mutations, represented by the *l7Rn5*^{3345SB} null allele and the *l7Rn5*^{1989SB} hypomorphic allele, disrupted EED interaction with HDACs and EZH2 (Denisenko et al., 1998; Sewalt et al., 1998; van Lohuizen et al., 1998; van der Vlag and Otte, 1999). A pivotal role for EED in PRC2/3/4 function was evident from global H3-K27 methylation defects in *eed* mutant embryonic and trophoblast stem cells (Montgomery et al., 2005). Homozygosity for the *l7Rn5*^{3345SB} null allele caused embryonic lethality and anteroposterior (AP) patterning defects of the primitive streak at gastrulation (Faust et al., 1995; Faust et al., 1998). By contrast, animals homozygous for the *l7Rn5*^{1989SB} hypomorphic allele were viable and manifested highly penetrant, dosage-sensitive posterior homeotic transformations along the vertebral column, as well as ectopic Hox gene expression (Schumacher et al., 1996; Wang et al., 2002). Additional developmental functions of EED included the regulation of random and imprinted X chromosome inactivation (Wang et al., 2001; Mak et al., 2002; Plath et al., 2003; Silva et al., 2003; Kalantry and Magnuson, 2006; Kalantry et al., 2006) and genomic imprinting (Mager et al., 2003). Furthermore, *eed* mutant animals exhibited hematopoietic defects in the bone marrow and thymus (Lessard et al., 1999; Richie et al., 2002).

Surprisingly, despite a significant overlap in homeotic phenotypes and co-regulation of Hox genes, the present genetic analysis implicated *eed* and *Bmi1* in parallel pathways, which converged at the level of Hox gene regulation. EED and BMI1 engaged in separate, but juxtaposed complexes at Hox target loci. While both complexes contain YY1 as a DNA-binding factor, EED, but not BMI1, associated with methylated H3-K27. The combined genetic, biochemical and molecular results form the basis for a model of PcG complex recruitment and retention in mammalian Hox gene clusters.

MATERIALS AND METHODS

Mouse strains and genotyping

l7Rn5^{3345SB} and *l7Rn5*^{1989SB} represent *eed* null and hypomorphic alleles, respectively, generated by *N*-ethyl-*N*-nitrosourea mutagenesis (Schumacher et al., 1996; Rinchik and Carpenter, 1999). The T^{1040}→C transition in the *l7Rn5*^{3345SB} allele disrupted a diagnostic *Alu*I site used for genotyping (Schumacher et al., 1996). PCR amplification with primers 5′-GTT-GGCCATGGAAATGTTA (forward) and 5′-CTATGCATTCTCAGAA-CAC (reverse) created a diagnostic *Mse*I site in the context of the T^{1031}→A transversion in the *l7Rn5*^{1989SB} allele. The *Bmi1* null mutation was generated by gene targeting and detected by PCR as reported (van der Lugt et al., 1994). All mice were on a partially congenic FVB/NJ background (N5). For the developmental studies, embryos were recovered at embryonic day (E) 8.5 or 12.5 from timed matings. Noon of the day of the appearance of the vaginal plug was considered E0.5.

Skeletal preparations

Whole-mount preparations of P0 skeletons were stained with 0.015% Alcian Blue 8GX (Sigma) and 0.005% Alizarin Red S (Sigma) and cleared by alkaline digestion in potassium hydroxide for 7-10 days as described previously (van der Lugt et al., 1994).

Immunohistochemistry and mRNA in situ hybridization

Immunohistochemistry and streptavidin-biotin immunoperoxidase detection on parasagittal 5 μm sections from E12.5 embryos were performed as described recently (Mok et al., 2004). mRNA in situ hybridization to parasagittal 7 μm sections from E12.5 embryos was conducted according to a standard protocol with minor modifications (Neubüser et al., 1995). Depending on the expression level, the alkaline phosphatase reaction was extended up to 4 weeks with weekly changes of the substrate solution to enhance signal intensity.

Digoxigenin-11-UTP-labeled antisense cRNA probes were prepared as reported (Wilkinson and Nieto, 1993). Antisense cRNA probes were generated from plasmids described previously: *eed* (Faust et al., 1995), *Hoxa5* (Colberg-Poley et al., 1985), *Hoxa7* (Yu et al., 1995), *Hoxb3* (Sham et al., 1992), *Hoxb4* (Ramirez-Solis et al., 1993), *Hoxb6* (Schughart et al., 1988) and *Hoxd4* (Gaunt et al., 1989). In addition, a 408 base pair (bp) *Hoxc8* probe (corresponding to nucleotides 274-682 of GenBank Accession number NM010466) and a 741 bp *Bmi1* probe (corresponding to nucleotides 1529-2270 of GenBank Accession number XM130022) were employed. Sense *eed* and *Bmi1* cRNA probes served as negative controls.

Whole-mount in situ hybridization was performed as described (Wilkinson and Nieto, 1993). The alkaline phosphatase detection reactions generally reached completion within 3 days. Images were captured from flat-mount preparations of embryos under coverslips.

Immunoprecipitation and western blot analysis

E12.5 embryos were dissected and eviscerated and limbs and heads were removed. The remaining trunks were pooled (n=2-3) and sonicated in lysis buffer [20 mmol/l Tris pH 7.5, 150 mmol/l NaCl, 1 mmol/l EDTA, 1 mmol/l EGTA, 1% Triton X-100 with Complete Mini Protease Inhibitor (Roche)]. Two milligrams of protein lysate were incubated overnight with an α-Eed or α-Bmi1 antibody covalently coupled to beads [ProFound Mammalian Co-Immunoprecipitation Kit (Pierce)] or with an α-Bmi1 antibody preincubated with protein G/A agarose beads (Oncogene). As a control, lysates were incubated with free beads. Elutions were separated on SDS-PAGE gels and transferred onto PVDF membrane (BioRad) for western blot analysis. Membranes were blocked with 5% BSA in TBST (20 mmol/l Tris, pH 7.6, 137 mmol/l NaCl, 0.1% Tween-20) or ReliaBlot reagent (Bethyl Laboratories) for 2 hours at room temperature and incubated overnight at 4°C with α-EED, α-BMI1, α-RING1B, α-EZH2, α-H3M2K27, or α-YY1 antibody. Following incubation with appropriate horseradish

peroxidase-conjugated secondary antibodies, (co-)immunoprecipitated proteins were detected by chemiluminescence (ECL reagent, Santa Cruz Biotechnology).

Chromatin immunoprecipitation

Chromatin immunoprecipitation (ChIP) was performed with the ChIP Assay Kit (Upstate). Input consisted of eviscerated E12.5 embryos without limbs and heads. For spatial analysis of EED and BMI1 binding to Hox regulatory regions, trunks were dissected further and cut rostral to the anterior expression boundaries of *Hoxa5* (pv3) or *Hoxc8* (pv12). Pools of two to three entire trunks, or pools of five to ten anterior and posterior fragments were incubated in 1% formaldehyde for 10 minutes at 37°C. Following crosslinking, tissues were washed and sonicated to shear the DNA to lengths between 200 and 1000 bp. Sonicated supernatants were precleared with salmon sperm DNA/protein A (or protein G) agarose beads, and incubated overnight with approximately 5 μg antibody. The chromatin-antibody complex was collected with salmon sperm DNA/protein A (or protein G) agarose. Crosslinking was reversed with sodium chloride at 65°C overnight. Phenol:chloroform-extracted chromatin was employed for PCR amplification of Hox promoter sequences. *Hoxa5:* 5′-CGTAACCGTCAGTGGGAGA (forward) and 5′-GGAATCATTTCGTGGCTGTG (reverse), 5′-ACCCAACTCCCCCATTAGTG and 5′-TGTGCTTGATTTGTGGCTCG (reverse). *Hoxc8*: 5′-TGAGCACAATAGCCCACACG (forward) and 5′-TGGGAGAACCTGAGAGCAAAG (reverse), 5′-GCCCTGACTTACTAACTCTCACCTC (forward) and 5′-GCTCTCTGCTCACTGTCGGTAG (reverse). The promoter region of β-*actin* served as a negative control using primers 5′-ACAAGGGCGGAGGCTATTC (forward) and 5′-AGGCAACTTTCGGAACGG (reverse).

Antibodies

The following antibodies were employed: α-EED (rabbit polyclonal, raised against EED residues 123-140, custom-generated by Bethyl Laboratories), α-BMI1 antibody (rabbit polyclonal, raised against BMI1 residues 229-314, custom-generated by Bethyl Laboratories; mouse monoclonal, Upstate; goat polyclonal, Abcam; goat polyclonal, Santa Cruz Biotechnology), α-RING1B (mouse monoclonal, kindly provided by Haruhiko Koseki; rabbit polyclonal, Abcam), α-EZH2 (rabbit polyclonal, Upstate; rabbit polyclonal, Abcam; rabbit polyclonal, Bethyl Laboratories), α-H3M2K27 (rabbit polyclonal, Upstate), α-H3M3K27 (rabbit polyclonal, Upstate), α-YY1 (rabbit polyclonal, Abcam; rabbit polyclonal, Santa Cruz Biotechnology), and α-FPN1 (rabbit polyclonal, raised against residues 553-568 at the FPN1 carboxy terminus, custom-generated by Bethyl Laboratories; see also Mok et al. (Mok et al., 2006).

RESULTS

Coexpression of *eed* and *Bmi1* in somites and neuroectoderm

Previous reports, mostly based on northern analysis of adult tissues and cell lines, indicated widespread mRNA expression of *eed* and *Bmi1* (Schumacher et al., 1996; Alkema et al., 1997a; Denisenko and Bomsztyk, 1997; Gunster et al., 1997; Denisenko et al., 1998; Rietzler et al., 1998; Schumacher et al., 1998; Sewalt et al., 1998; Peytavi et al., 1999). mRNA in situ hybridization studies detected coexpression of *eed* and *Bmi1* in somites and neuroectoderm in E8.5 wild-type embryos (Fig. 1A,E). Likewise, at E12.5, prevertebrae and neuroectoderm exhibited coexpression of *eed* and *Bmi1* mRNA (Fig. 1B,F). Control experiments with *eed* and *Bmi1* sense probes revealed no signal on sectioned E12.5 embryos (Fig. 1C,G). Immunohistochemistry confirmed EED and BMI1 protein expression in the nuclei of E12.5 prevertebrae (Fig. 1D,H).

eed×*Bmi1* double mutant mice

Crosses between *eed* heterozygotes, i.e. $l7Rn5^{3345SB/+}$ or $l7Rn5^{1989SB/+}$, with *Bmi1* heterozygotes, followed by inter se crosses of double heterozygotes, yielded the various double mutant genotypes for this study. Homozygosity for the $l7Rn5^{3345SB}$ allele caused lethality at gastrulation (Faust et al., 1995), whereas $l7Rn5^{1989SB}$ homozygotes were viable and fertile (Schumacher et al., 1996). Consequently, results from *eed* homozygotes at E12.5 and P0 encompassed the $l7Rn5^{1989SB}$ allele. Twenty percent of the *eed*;*Bmi1* double homozygotes survived to term, but the severely runted pups died invariably during the first 24 hours. All other genotypes segregated with the expected Mendelian ratio and resulted in viable offspring (data not shown).

$l7Rn5^{3345SB}$ or $l7Rn5^{1989SB}$ heterozygotes presented no significant difference in the penetrance of homeotic transformations and ectopic Hox gene expression in *trans* with *Bmi1* heterozygosity or homozygosity (data not shown). In the absence of allele-specific effects, data for $l7Rn5^{3345SB}$ and $l7Rn5^{1989SB}$ were combined. These results also suggested haploinsufficiency of the $l7Rn5^{1989SB}$ allele in the homeotic pathways, which contrasted with its dominant-negative function in carcinogen-induced T-cell lymphoma development (Richie et al., 2002).

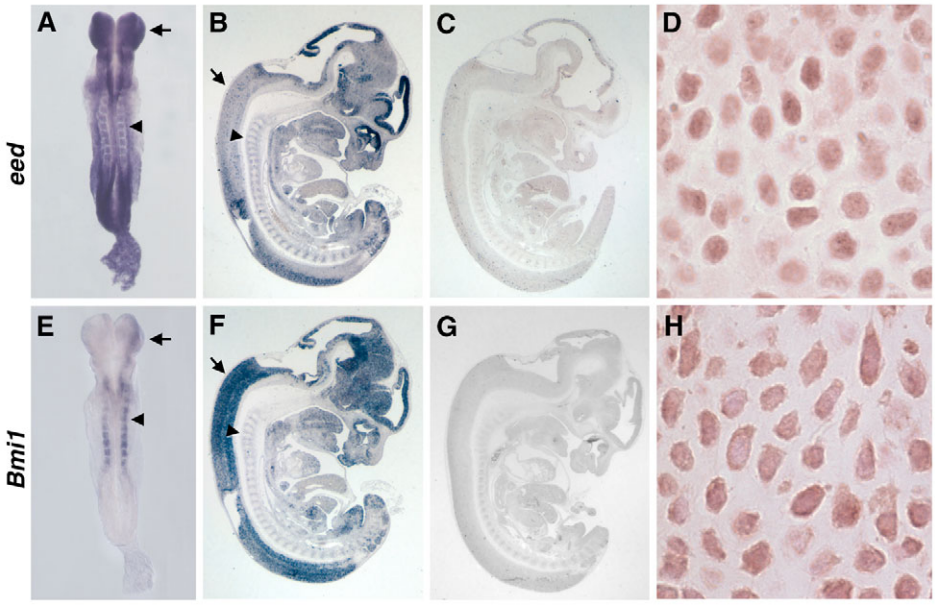

Fig. 1. Coexpression of *eed* and *Bmi1* in wild-type embryos. Representative images of flat-mount E8.5 embryos (**A**,**E**) and sectioned E12.5 embryos (**B**,**F**) mRNA in situ hybridization with *eed* (A,B) and *Bmi1* antisense cRNA probes (E,F). Note coexpression of *eed* and *Bmi1* mRNA in somites (arrowheads in A,E) and prevertebrae (arrowheads in B,F), as well as neuroectoderm (arrows in A,B,E,F). Control hybridization with *eed* and *Bmi1* sense cRNA probes revealed no specific signal on sectioned E12.5 embryos (**C**,**G**). Immunohistochemistry detected nuclear expression of EED and BMI1 in E12.5 prevertebrae (**D**,**H**). The images were captured at 20× (B,C,F,G), 50× (A,E), and 1000× (D,H).

eed and *Bmi1* function additively in the regulation of vertebral identity

Analysis of whole-mount skeletal preparations provided a powerful means for quantitative characterization of the functional relationship between *eed* and *Bmi1* in axial patterning. By genetic criteria, the overlapping, dosage-sensitive transformations in *eed* and *Bmi1* single mutants (van der Lugt et al., 1994; Schumacher et al., 1996) reflect a common, sensitized pathway(s) susceptible to changes in phenotypic penetrance and expressivity in the presence of a non-allelic modifier. Synergistic interaction between *eed* and *Bmi1* would manifest as supra-additive increases in the penetrance of axial transformations, as well as expression of novel phenotypes, similar to *Bmi1*;*M33* double mutants (Bel et al., 1998). Alternatively, in case of sole dependence of PRC1 recruitment on PRC2/3/4-mediated methylation of H3-K27 (Cao et al., 2002; Czermin et al., 2002; Kuzmichev et al., 2002; Müller et al., 2002; Wang, L. et al., 2004; Cao et al., 2005), *eed*;*Bmi1* double mutants would exhibit the *eed* single mutant phenotype.

Fig. 2A summarizes the results of 668 skeletal preparations comprising all nine genotypes obtained from *eed*;*Bmi1* double heterozygous intercrosses. In agreement with previous studies (van der Lugt et al., 1994; Schumacher et al., 1996), mutant skeletons exhibited dosage-sensitive, posterior transformations along the entire AP axis, which ranged between 70 and 100% in *eed* and *Bmi1* homozygotes (Fig. 2A). Strikingly, the penetrance of the skeletal transformations in *eed*;*Bmi1* double heterozygotes reflected a strictly additive effect of the single heterozygous phenotypes (Fig. 2A). For example, the L6→S1 transformation was detected in 25 and 27% of $eed^{+/-}$;+/+ and +/+;$Bmi1^{+/-}$ skeletons, respectively, compared with 54% in double heterozygotes.

The penetrance of all homeotic transformations approached 100% in $eed^{-/-}$;$Bmi1^{-/-}$ double homozygotes (Fig. 2A). Although this hindered the evaluation of potential supra-additive increases in penetrance, changes in phenotypic expressivity, another hallmark of synergistic genetic interaction, could readily be ascertained. Regardless of the severity of the double mutant genotype, the transformations remained restricted to individual axial segments and were phenotypically identical to those detected in *eed* and *Bmi1* single mutants (Fig. 3C-G). This included the cervical region, which represented a focal point of *M33*×*Bmi1* synergy and manifested transformations across multiple vertebrae (Bel et al., 1998). Furthermore, two ectopic ossification centers rostral to the first cervical vertebra and broadening of the neural arch of C1 in *Bmi1* homozygotes represented known *Bmi1*-specific defects (van der Lugt et al., 1994) with phenotypic expression not enhanced by *eed* mutant alleles (Fig. 3C,D). Finally, unlike crosses between *M33* and *Bmi1*, the axial and appendicular skeleton in *eed*;*Bmi1* double mutants did not present any novel phenotypes compared with the single mutants and wild-type controls (data not shown).

Thus, by contrast to intercrosses of PRC1 mutant alleles, genetic interaction between constituents of PRC1 and PRC2/3/4 did not result in synergistic phenotypes. The double mutant phenotype also rendered sole dependence of PRC1 recruitment on PRC2/3/4-mediated methylation of H3-K27 unlikely. Rather, in the context of a sensitized PcG pathway(s), additive increases in the penetrance of homeotic transformations are most consistent with parallel function of EED and BMI1 in the regulation of vertebral identity.

eed and *Bmi1* regulate an overlapping set of Hox genes

To account for the haploinsufficiency of *eed* and *Bmi1* function, as well as to detect potential cross- and para-regulatory interferences of Hox gene transcription (Gould et al., 1997; Mann, 1997), 237 embryos encompassing all nine *eed*×*Bmi1* genotypes yielded sections for 352 mRNA in situ hybridizations (Fig. 2B,

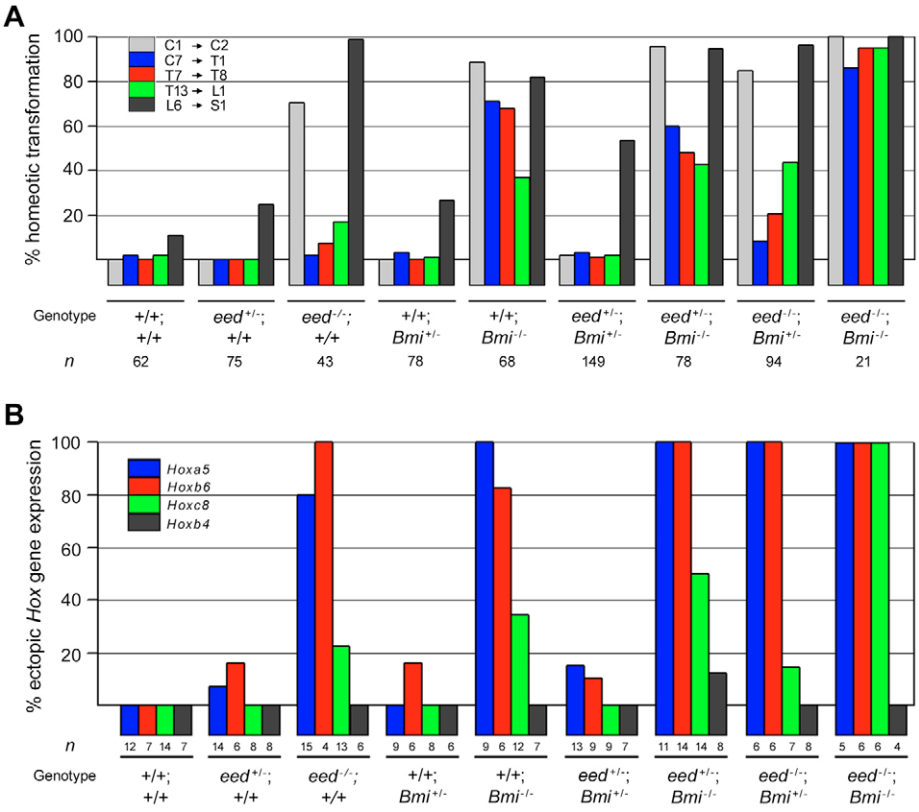

Fig. 2. Homeotic transformations and ectopic Hox gene expression in *eed*×*Bmi1* mutants. (**A**) The chart summarizes the penetrance of posterior homeotic transformations in P0 skeletons. The inset depicts the color-coding of the five transformations assessed. The columns represent the percentage of skeletons exhibiting the cervical (C), thoracic (T), lumbar (L) or sacral (S) transformations. Unilateral and bilateral transformations were combined. See the legend for Fig. 3 for a description of the transformations. The genotypes and the number (*n*) of skeletons analyzed per genotype are shown at the bottom of the figure. (**B**) The chart summarizes the penetrance of ectopic Hox gene expression in prevertebrae of E12.5 embryos. The inset depicts the color-coding of the four Hox genes tested (*Hoxa5*, *b6*, *c8* and *b4*). The columns indicate the percentage of embryos exhibiting ectopic Hox gene expression. The genotypes and the number (*n*) of embryos analyzed per genotype and Hox probe are shown below the columns.

Fig. 3A,B). In agreement with previous reports (Gaunt, 1988; Dressler and Gruss, 1989; Gaunt et al., 1989; Gaunt et al., 1990; Kessel and Gruss, 1991; Sham et al., 1992; Eid et al., 1993; Akasaka et al., 1996), the following anterior boundaries of high-level Hox gene expression were detected in the prevertebrae (pv) of E12.5 embryos: pv3 (*Hoxa5*), pv10 (*Hoxa7*), pv1 (*Hoxb3*), pv2 (*Hoxb4*), pv7 (*Hoxb6*), pv12 (*Hoxc8*) and pv2 (*Hoxd4*) (Fig. 3A,B and data not shown). Likewise, discrete levels of *Hoxa5, Hoxb4* and *Hoxd4* expression were frequently detected in the prevertebra directly rostral to the anterior boundary (Fig. 3A,B and data not shown).

Compared with wild-type littermates, E12.5 *eed* mutant embryos displayed ectopic expression of *Hoxa5*, *Hoxb3*, *Hoxb6* and *Hoxc8* in prevertebrae, whereas *Hoxa7*, *Hoxb4* and *Hoxd4* expression appeared unaffected (Fig. 2B, Fig. 3A,B and data not shown). Therefore, EED functions as a negative regulator of Hox gene

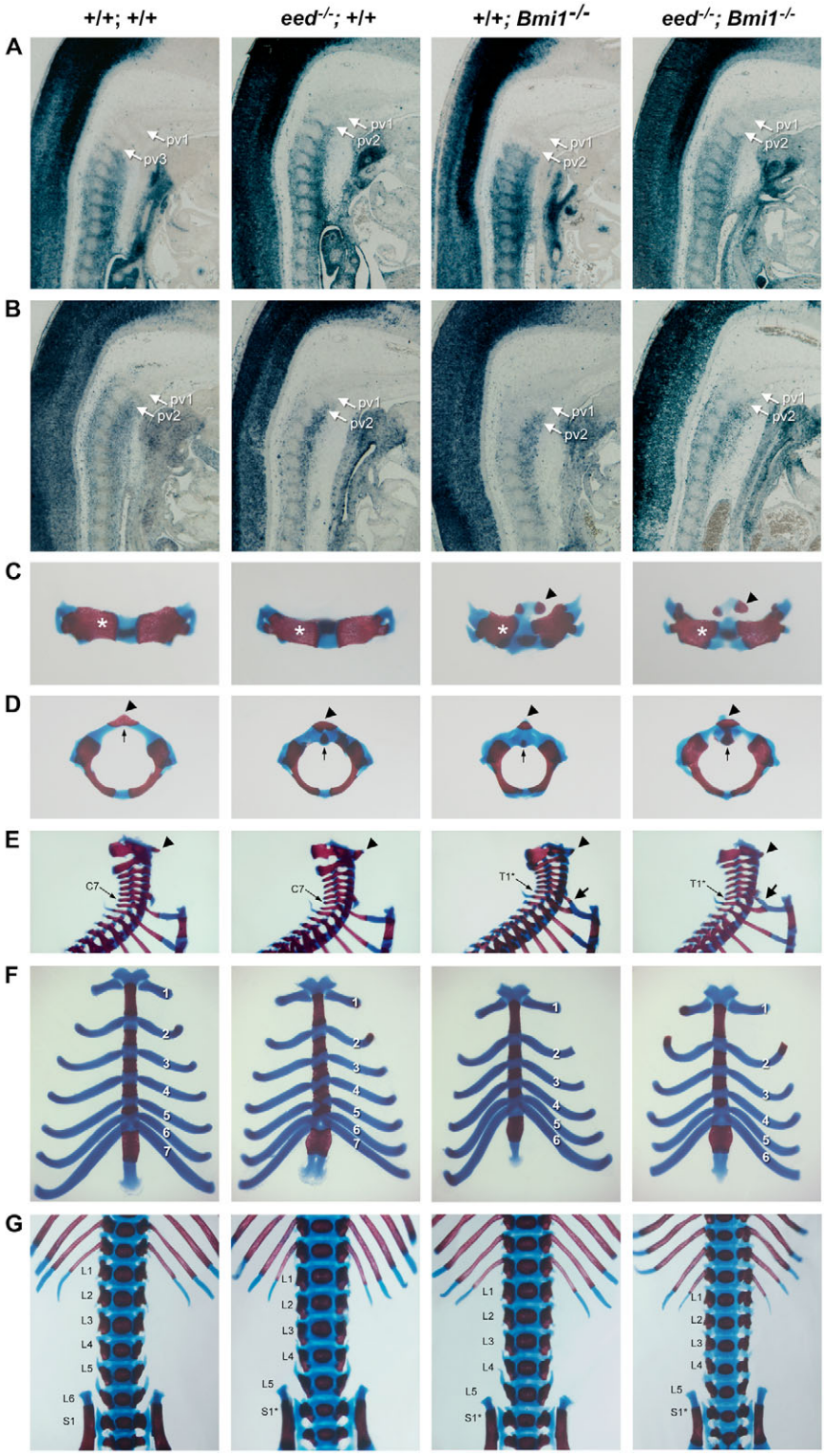

Fig. 3. Ectopic Hox gene expression and skeletal analysis in *eed*×*Bmi1* mutants. Genotypes are indicated above the panels. (**A**,**B**) Representative images of sectioned wild-type and mutant embryos following mRNA in situ hybridization with *Hoxa5* (A) and *Hoxb4* (B) antisense probes. Arrows denote the anterior Hox gene expression boundary and the first prevertebra. All images were captured at 50× magnification. (**C-G**) Homeotic transformations and vertebral abnormalities in cervical (C-E), thoracic (F) and lumbar regions (G). (C) Two ectopic ossification centers (arrowheads) and broadening of the neural arch (asterisk) constitute *Bmi1*-specific defects (van der Lugt et al., 1994). (D) The first cervical vertebra reveals a significantly broader ventral arch in *eed* and *Bmi1* mutant skeletons (arrow), which is likely to result from an incomplete regression of the vertebral body during embryogenesis (Verbout, 1985). As all vertebrae posterior to C1 contain a body, incomplete regression of the body in C1 represents a posterior homeotic transformation (C1→C2). (D,E) The rudimentary vertebral body also broadens the anterior arch, which is visible in both rostral and lateral views of C1 (arrowheads). (E) The presence of ribs transforms the seventh cervical vertebra toward the identity of the first thoracic vertebra (C7→T1*). (F) Posterior transformation of the seventh thoracic vertebra is evident from lack of sternal fusion of the ribs (T7→T8). (G) Fusion with the ilial bones represents a homeotic transformation of the sixth lumbar vertebra toward a sacral identity (L6→S1*). Images were captured at 20× (C,D), 16× (E), 12× (F) and 18× magnification (G). pv, prevertebra.

transcription, corroborating a previous study in E11.5 embryos (Wang et al., 2002). To ascertain a potential role for EED in early Hox gene repression, the expression of *Hoxa5* and *Hoxb6* was examined by whole-mount in situ hybridization in E8.5 *eed* mutant embryos (Fig. 4). *l7Rn5*$^{1989SB/1989SB}$ and wild-type embryos presented the same anterior *Hoxa5* and *Hoxb6* expression boundary at the level of somites 5 and 8, respectively. These results contrasted with ectopic *Hoxa5* and *Hoxb6* expression in *l7Rn5*$^{1989SB/1989SB}$ embryos at E12.5 (Fig. 2B). Thus, similarly to *Bmi1* and other *PcG* genes, EED is required for maintenance but not initiation of Hox gene expression.

In agreement with previous studies (van der Lugt et al., 1996; Bel et al., 1998), +/+;*Bmi1*$^{-/-}$ embryos manifested ectopic expression of *Hoxa5*, *Hoxb6* and *Hoxc8* (Fig. 2B, Fig. 3A,B). This contrasted with downregulation of *Hoxb6* as well as normal expression levels of *Hoxa5* and *Hoxc8* in *Bmi1*-deficient murine embryonic fibroblasts (MEFs) (Cao et al., 2005) and suggests changes in PcG-mediated repression in response to cellular differentiation. Four Hox probes were selected for the analysis in *eed*;*Bmi1* double mutants based on the presence (*Hoxa5*, *Hoxb6*, *Hoxc8*) or absence (*Hoxb4*) of ectopic expression in the single mutants. As shown in Fig. 2B, the penetrance of ectopic *Hoxa5*, *Hoxb6* and *Hoxc8* expression increased with the severity of the genotype and reached 100% in *eed*;*Bmi1* double homozygotes. By contrast, the phenotypic expressivity was unaffected and ectopic expression remained confined to a single prevertebra rostral to the wild-type anterior expression boundary (Fig. 2B, Fig. 3A and data not shown). Furthermore, ectopic *Hoxb4* expression was not detected, regardless of the genotypic severity (Fig. 2B, Fig. 3B).

In conclusion, additive effects in genetically sensitized double heterozygotes, confinement of ectopic Hox gene expression and homeotic transformations to single segments, and absence of novel phenotypes strongly support the notion that *eed* and *Bmi1* govern parallel pathways converging at the level of Hox gene regulation.

EED and BMI1 form separate protein complexes in embryos

An antibody raised against residues 123-140 of the EED amino terminus precipitated three distinct isoforms of approximately 50 and 75 kDA from E12.5 trunk (Fig. 5), representing three of the four EED isoforms previously reported in 293 cells (Kuzmichev et al., 2004). In addition to EZH2 and YY1, dimethylated H3-K27 co-immunoprecipitated with EED (Fig. 5). Immunoprecipitation

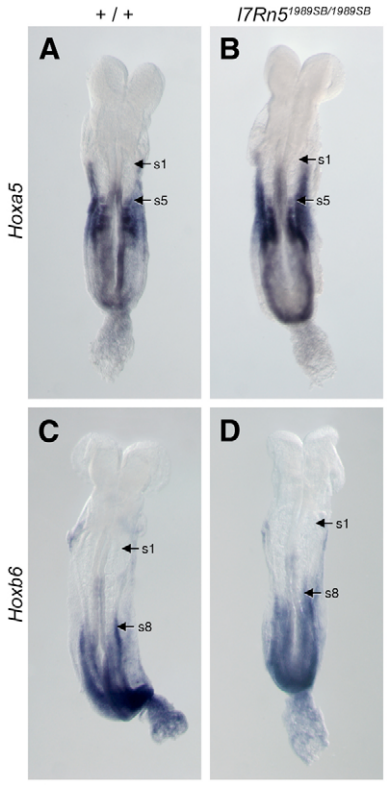

Fig. 4. Normal Hox gene expression in E8.5 eed mutant embryos. Representative flat-mount images of wild-type (**A**,**C**) and *l7Rn5*$^{1989SB/1989SB}$ mutant embryos (**B**,**D**) following mRNA in situ hybridization with *Hoxa5* (A,B) and *Hoxb6* (C,D) antisense cRNA probes. Note that wild-type and *l7Rn5*$^{1989SB/1989SB}$ mutant embryos present the same anterior Hox gene expression boundaries in somites (s). Arrows denote the first somite and the anterior Hox gene expression boundary. All images were captured at 50× magnification.

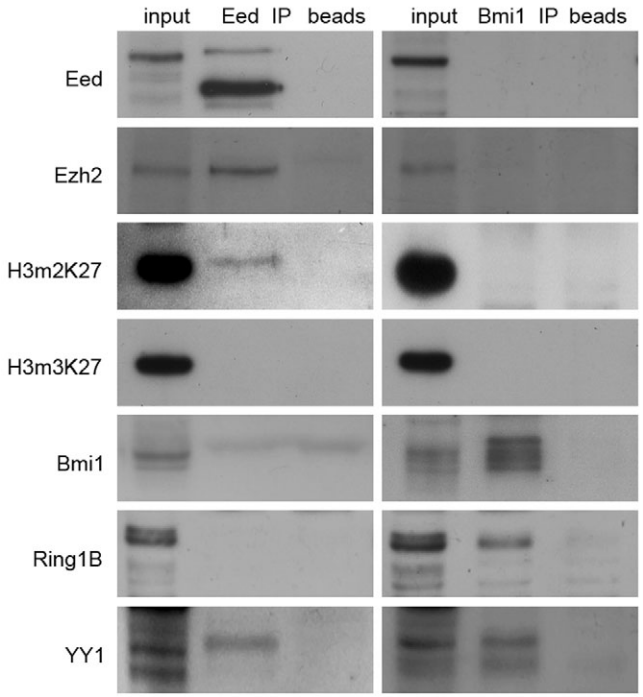

Fig. 5. EED and BMI1 engage in separate protein complexes. Immunoprecipitation of EED (left column) from E12.5 trunk identified three isoforms of approximately 50 and 75 kDA. Note the absence of the EED isoforms in the input lane, indicating low levels of EED expression. EED co-immunoprecipitated with EZH2 and dimethylated H3-K27, which presented a molecular weight of approximately 100 and 17 kDA, respectively. Immunoprecipitation of BMI1 (right column) from E12.5 trunk revealed three isoforms in the 39-41 kDA range. A fourth band, slightly larger than the triplet, was occasionally detected in mock immunoprecipitation without the BMI1 antibody and, hence, could not be confirmed as a BMI1 isoform. RING1B co-immunoprecipitated with BMI1 as a band of approximately 38 kDa. Note that reciprocal co-immunoprecipitation did not detect EED and BMI1 in a common protein complex, and trimethylated H3-K27 did not pull down with either complex. YY1, as a band of 49 kDA, co-immunoprecipitated with both EED and BMI1. IP, immunoprecipitation; beads, mock immunoprecipitation without antibody; input, 2 μg protein lysate; H3M2K27, dimethylated histone 3-K27, H3M3K27, trimethylated histone 3-K27.

identified three BMI1 isoforms of approximately 39-41 kDA. BMI1 was found in a complex with RING1B, but not dimethylated H3-K27. Similar to the EED complex, the BMI1 complex also contained YY1 (Fig. 5). It should be emphasized that all (co-)immunoprecipitating bands were detected by at least two antibodies against different epitopes. Strikingly, while dimethylated H3-K27 engaged in the EED complex, trimethylated H3-K27 did not appear to associate with either the EED or the BMI1 complex. Importantly, reciprocal co-immunoprecipitation detected EED and BMI1 in separate protein complexes.

Juxtaposition of EED and BMI1 chromatin complexes in Hox regulatory regions

Ectopic expression in mutant embryos revealed *Hoxc8* and *Hoxa5* as downstream targets of EED and BMI1 function (Fig. 2B, Fig. 3A). ChIP detected EED and BMI1 binding immediately upstream of the *Hoxc8* transcribed region near putative promoter elements (Fig. 6A,B). The binding sites could not be separated, indicating close proximity of the complexes (data not shown). EED and BMI1 binding also clustered within a small fragment 1.5 kb upstream of the *Hoxc8* transcription start site (Fig. 6A,B), suggesting long-range juxtaposition of heterologous PcG complexes. Similar to EED and BMI1, YY1 localized to both regions. In support of YY1 binding to Hox regulatory regions, inspection of the mouse genome sequence (NCBI Build 35) revealed clusters of putative YY1 binding sites in both regions a and b, including TGTCCATTAG and CCCCCATTCC (region a), as well as ACACCATGGC, TTTCCATTAG and TCCCCATAAA (region b). CCAT represents the core of the YY1 consensus binding site, while flanking sequences exhibited significant tolerance for multiple nucleotides (Shrivastava and Calame, 1994; Mihaly et al., 1998). EED, BMI1 and YY1 also co-localized approximately 1.5 kb upstream of the transcription start site of *Hoxa5* (Fig. 6B). In addition to PcG binding, ChIP detected trimethylated H3-K27 throughout the regulatory regions of *Hoxc8* and *Hoxa5* (Fig. 6B). Furthermore, dimethylated H3-K27 localized to region b of *Hoxc8*. The presence of the dimethylated histone domain in other regions could not be determined conclusively. ChIP using an antibody against ferroportin 1, a membrane-bound iron exporter (Mok et al., 2004), confirmed the specificity of the experiments and yielded no amplification of *Hoxc8* and *Hoxa5* genomic fragments (Fig. 6B). As an additional control, EED and BMI1 complexes did not localize to the β-*actin* promoter. Conversely, ChIP detected YY1 at the β-*actin* promoter, which contained a putative YY1 binding site CACCCATCGC. This finding is consistent with a context-dependent role of YY1 as a transcriptional activator (Gordon et al., 2006).

Spatial regulation of EED and BMI1 binding to Hox regulatory regions was evident from ChIP analysis of dissected anterior and posterior regions of E12.5 trunk. In agreement with transcriptional silencing of *Hoxc8* and *Hoxa5*, EED and BMI1 binding was detected upstream of these loci in anterior regions of the trunk (Fig. 6C). By contrast, EED and BMI1 binding was absent from posterior regions of the trunk, where *Hoxc8* and *Hoxa5* are transcribed. These findings implicate PcG complexes in Hox gene repression in anterior regions of the AP axis, consistent with a recent study (Fujimura et al., 2006).

The combined interpretation of the co-immunoprecipitation and ChiP results indicates that trimethylated H3-K27 did not form a complex with EED or BMI1, despite co-localization of the three proteins in Hox regulatory regions. By contrast, co-immunoprecipitation demonstrated physical association of the EED complex with dimethylated H3-K27. In aggregate, the results support a model in which EED- and BMI1-containing chromatin remodeling complexes exist as separate, but juxtaposed, biochemical entities at Hox target loci.

DISCUSSION

While recent years have witnessed significant progress in elucidating PcG complex interaction in *Drosophila* development and mammalian cell lines (Francis and Kingston, 2001; Lund and van

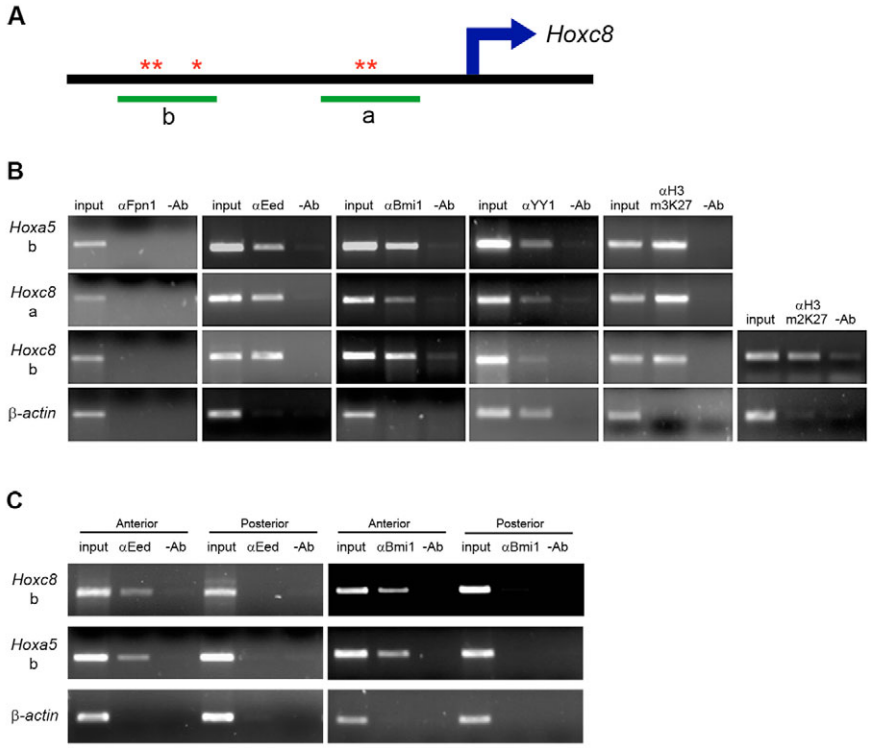

Fig. 6. Juxtaposition of EED and BMI1 complexes at Hox target loci. (**A**) A schematic representation of the *Hoxc8* upstream region is shown. The blue arrow depicts the *Hoxc8* transcription start site, and the green lines demark two upstream regions identified by ChIP located immediately upstream (a) and 1.5 kb upstream (b) of the *Hoxc8* transcription start site. Red asterisks indicate putative YY1-binding sites. (**B**) ChIP using antibodies against EED, BMI1, YY1 and trimethylated H3-K27 detected the proteins at the two upstream regions (a and b) of the *Hoxc8* locus. While dimethylated H3-K27 localized to region b of the *Hoxc8* locus, results for region a were variable and, hence, inconclusive. EED, BMI1, YY1 and trimethylated H3-K27 were also detected 1.5 kb upstream of the *Hoxa5* transcription start site. ChIP using an antibody against Fpn1 served as a negative control. (**C**) ChIP detected differential binding of EED and BMI1 binding to Hox regulatory regions in dissected anterior and posterior regions of E12.5 trunk. In all cases, input encompassed 1% of the chromatin used for ChIP, and mock ChIP without antibody served as additional negative controls. As a negative control, EED and BMI1 did not associate with the β-*actin* promoter.

Lohuizen, 2004; Ringrose and Paro, 2004), little is known about their functional interdependency in Hox gene regulation in the mouse embryo. Consistent with a common temporal requirement for PRC1 and PRC2/3/4, the present study demonstrated EED function in maintenance but not initiation of Hox gene repression, similar to BMI1/MEL18 and RAE28 (Tomotsune et al., 2000; Akasaka et al., 2001). *eed* and *Bmi1* single mutants revealed ectopic expression of a similar set of Hox genes and common posterior transformations. Notably, this represented the most significant overlap in molecular and vertebral phenotypes among the murine *PcG* genes analyzed thus far, including the BMI1 homolog MEL18 (van der Lugt et al., 1994; Akasaka et al., 1996; Schumacher et al., 1996; van der Lugt et al., 1996; Coré et al., 1997; Takihara et al., 1997; Katoh-Fukui et al., 1998; del Mar Lorente et al., 2000; Suzuki et al., 2002; Voncken et al., 2003; Isono et al., 2005). The distinct similarities in EED and BMI1 phenotypes predicted strong genetic interaction in double mutant crosses. Indeed, mutant alleles of *Drosophila Psc* significantly enhanced the homeotic phenotypes in $esc^{+/-}$ embryos devoid of maternal *esc* (Campbell et al., 1995).

Surprisingly, the present study revealed additive increases in the penetrance of homeotic transformations in *eed*;*Bmi1* double heterozygotes compared with the single mutants. Furthermore, regardless of the severity of the *eed*;*Bmi1* genotype, ectopic Hox gene expression and homeotic transformations remained confined to single segments, and novel phenotypes were not detected. Conceivably, compensatory activity by PcG paralogs could mask synergistic interactions in *eed*;*Bmi1* double mutants. Whereas the mouse genome appears devoid of an EED homolog, BMI1 and MEL18 display 70% protein sequence identity. However, BMI1 and MEL18 exerted only partially overlapping functions during mouse development and co-regulated a similar, but not identical, set of Hox genes (van der Lugt et al., 1994; Akasaka et al., 1996; Akasaka et al., 2001). In addition, BMI1, but not MEL18, promoted the E3 ligase activity of RING1B in vitro (Cao et al., 2005). Most importantly, the same *Bmi1* allele employed in this study synergistically enhanced the deficiency for *M33* (Bel et al., 1998), rendering compensatory activity of MEL18 unlikely. Furthermore, the *Bmi1*;*M33* double mutant crosses provide testimony to the inherent capacity of the mammalian PcG repressor system to express synergistic phenotypes upon mutational disruption.

The genetic interaction between *eed* and *Bmi1* in the regulation of vertebral identity also differs from studies in *Drosophila* embryos and mammalian cell lines, which suggest hierarchical PcG complex recruitment (Cao et al., 2002; Czermin et al., 2002; Kuzmichev et al., 2002; Müller et al., 2002; Wang, L. et al., 2004; Cao et al., 2005). Genetically, this should render the phenotypes of *eed*;*Bmi1* double mutants indistinguishable from the *eed* single mutants. Therefore, rather than a synergistic or strictly hierarchical interplay of the core PcG complexes in the regulation of vertebral identity, the genetic interaction between *eed* and *Bmi1* mutant alleles is most consistent with parallel pathways converging at the level of Hox gene repression.

Toward elucidation of the molecular mechanisms governing PcG pathway convergence, co-immunoprecipitation detected EED and BMI1 in separate complexes with EZH2 and RING1B, respectively, consistent with formation of PRC2/3/4 and PRC1 at E12.5. Interestingly, the zinc finger transcription factor YY1 co-immunoprecipitated with both EED and BMI1, suggesting developmental co-existence of YY1 in heterologous PcG core complexes. Previous studies in *Drosophila* and *Xenopus* embryos, as well as mammalian cell lines, revealed a context-dependent proclivity of YY1 to associate with constituents of PRC1 or PRC2/3/4 (García et al., 1999; Poux et al., 2001; Satijn et al., 2001; Levine et al., 2002; Mak et al., 2002; Atchison et al., 2003; Jin et al., 2003; Lorente et al., 2006). Direct support for mammalian YY1 as a PcG protein derived from axial homeotic transformations in *Yy1* mutant mice and genetic interaction with RING1A (Lorente et al., 2006).

Clusters of putative YY1/Pho DNA-binding sites have been detected near mammalian Hox genes as well as in *Drosophila* PREs (Brown et al., 1998; Fritsch et al., 1999; Mihaly et al., 1998; Gilthorpe et al., 2002). Indeed, EED, BMI1 and YY1 associated with DNA fragments at the *Hoxc8* and *Hoxa5* locus, which harbored several putative YY1-binding sites within fewer than 50 bp. This strongly supports the notion that YY1 bestows sequence-specific DNA binding on heterologous PcG complexes, and, by virtue of clustered YY1-binding sites, governs their juxtaposition in Hox regulatory regions in the mouse embryo. Interestingly, PLZF (promyelocytic leukaemia zinc finger) also binds to multiple *cis*-acting elements near Hox transcription units and interacts directly with BMI1 in vivo (Barna et al., 2002). Whether both PLZF and YY1 form a common complex with BMI1 or, alternatively, whether YY1 or PLZF interact with BMI1, depending on the Hox target locus, awaits investigation.

Juxtaposed EED and BMI1 complexes associated with DNA fragments immediately upstream of the transcribed regions of *Hoxc8* and *Hoxa5*. These findings are consistent with binding of both PcG complexes to the *Hoxc13* and *Hoxb8* promoter regions in MEFs and E12.5 mouse embryos, respectively (Cao et al., 2005; Fujimura et al., 2006). Furthermore, components of the general transcription machinery interact directly with constituents of PRC1, supporting a role for PcG targeting of the core promoter (Breiling et al., 2001; Saurin et al., 2001). Detection of EED and BMI1 complexes 1-1.5 kb upstream of the *Hoxc8* and *Hoxa5* transcribed regions could suggest looping of PcG complexes from the core promoter. Indeed, PLZF dimers or trimers form loops between several PLZF-binding sites in *Hoxd11* regulatory regions (Barna et al., 2002). In support of a similar mechanism, all DNA fragments associated with EED and BMI1 at the *Hoxc8* and *Hoxa5* locus harbor putative YY1-binding sites. However, to the best of our knowledge, formation of YY1 multimers has not been reported. Alternatively, the present results could implicate long-range PcG complex formation and histone modifications in Hox regulatory regions. Accordingly, multiple YY1-binding sites would anchor arrays of independent PcG complexes. In support of this notion, large continuous stretches of histone modifications across the Hox clusters contrast with punctate chromatin domains at reference loci (Bernstein et al., 2005). As an example for the unusual chromatin organization of the mammalian Hox clusters, a transcriptionally active chromatin domain governed by dimethylated H3-K4 spanned nearly 60 kb in length from *Hoxa1* to the *Hoxa7* locus. Conceivably, long-range assembly of PcG complexes might form equally large repressed chromatin domains across transcriptionally silent Hox genes in mouse embryos.

Consistent with the presence of stable heterochromatin domains, ChIP detected both di- and trimethylated H3-K27 in the vicinity of EED and BMI1 complex binding in Hox regulatory regions. Strikingly, while trimethylated H3-K27 did not appear to stably associate with either PcG complex, dimethylated H3-K27 co-immunoprecipitated with EED, but not BMI1, from E12.5 trunk. Thus, while methylated H3-K27 plays a pivotal role in PRC1 recruitment (Cao et al., 2002; Czermin et al., 2002; Kuzmichev et al., 2002; Müller et al., 2002; Wang, L. et al., 2004; Cao et al., 2005), it does not permanently associate with this complex at later

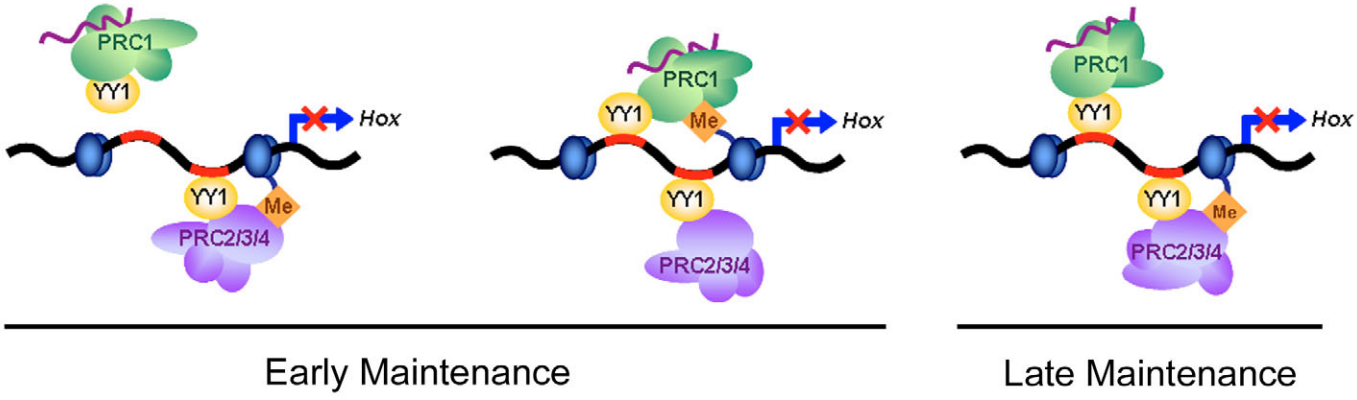

Fig. 7. Model of PcG complex assembly at Hox target loci. Nucleosomes and methylated H3-K27 are depicted as blue ovals and orange diamonds, respectively. Clustered YY1 binding sites are indicated in red. The purple line represents potential cooperative interactions between RNA molecules and PcG proteins. Based on previous PcG and trxG mutant analysis (Yu et al., 1995; Yu et al., 1998; Deschamps et al., 1999; Tomotsune et al., 2000), the transition from initiation to maintenance of Hox gene expression should occur between E9 and E10 of mouse development, herein referred to as 'Early Maintenance' phase. Complex assembly during the 'Late Maintenance' phase was ascertained from E12.5 embryos.

stages of Hox gene silencing. Beyond co-localization at potential target loci in mammalian embryonic stem cells and embryonic fibroblasts, as well as in *Drosophila* Kc and S2 cells (Boyer et al., 2006; Bracken et al., 2006; Lee et al., 2006; Schwartz et al., 2006; Tolhuis et al., 2006), the present study demonstrates direct physical interaction of PRC2/3/4 with dimethylated H3-K27 in differentiating somites. Therefore, at least in the context of Hox regulatory regions, the close proximity of PcG complexes and trimethylated H3-K27 does not equate to a stable physical association between PcG complexes and this modified histone site. Hence, defining the physical relationship between PcG complexes and histone sites at the recently identified target loci necessitates the complementation of the ChIP results by co-immunoprecipitation experiments in mouse embryos (Boyer et al., 2006; Bracken et al., 2006; Lee et al., 2006; Schwartz et al., 2006; Tolhuis et al., 2006).

The aggregate findings are depicted in a dynamic model of PcG complex assembly in mouse Hox gene clusters (Fig. 7). During the early maintenance phase of axial Hox gene repression, presumably between E9 and 10 (Yu et al., 1995; Yu et al., 1998; Deschamps et al., 1999; Tomotsune et al., 2000), PRC2/3/4 binds to Hox target loci via YY1 and methylates H3-K27. In turn, the H3-K27 mark serves as a binding site for PRC1 to Hox target loci. However, additive homeotic phenotypes in *eed*;*Bmi1* double mutants render sole dependence of PRC1 recruitment on methylated H3-K27 unlikely. Rather, YY1 binding sites, and as recently shown noncoding RNA molecules (Bernstein et al., 2006; Sanchez-Elsner et al., 2006), represent strong candidates for cooperative interaction with the H3-K27 mark in recruitment of PRC1 to target loci. Upon dissociation from methylated H3-K27, possibly governed by conformational changes, PRC1 retention at Hox regulatory regions would predominantly depend on YY1-mediated DNA binding. Juxtaposed PRC2/3/4, bound to DNA via YY1, stably re-associates with dimethylated H3-K27 throughout the maintenance phase of Hox gene repression and somite differentiation. In support of this notion, two recent studies demonstrated that PRC2/3/4-mediated methylation of H3-K27 prevents reactivation of silenced target loci during cellular differentiation (Kalantry and Magnuson, 2006; Kalantry et al., 2006). Thus, the model implicates a cooperative interplay between epigenetic and genetic elements in the recruitment and retention of juxtaposed PcG complexes in mammalian Hox gene clusters, delineating a molecular definition of PcG pathway convergence in the regulation of vertebral identity.

The authors are grateful to Maarten van Lohuizen for generously providing the *Bmi1* mutant mice, as well as critical reading of the manuscript. Jacqueline Deschamps, Denis Duboule, Peter Gruss, Stanley Korsmeyer and Robb Krumlauf kindly provided the plasmids for the Hox probes. We thank Haruhiko Koseki for the RING1B antibody, Thomas Guenther for help with mRNA in situ hybridization, and Gerard Karsenty for access to microscopes and imaging equipment. S.Y.K. received partial support from a NIGMS predoctoral training grant. This work was supported by grants from the NIH, the Merck Genome Research Institute and the Curtis Hankamer Basic Research Fund to A.S.

References

Adler, P. N., Charlton, J. and Brunk, B. (1989). Genetic interactions of the *suppressor 2 of zeste* region genes. *Dev. Genet.* **10**, 249-260.
Adler, P. N., Martin, E. C., Charlton, J. and Jones, K. (1991). Phenotypic consequences and genetic interactions of a null mutation in the *Drosophila Posterior Sex Combs* gene. *Dev. Genet.* **12**, 349-361.
Akasaka, T., Kanno, M., Balling, R., Mieza, M. A., Taniguchi, M. and Koseki, H. (1996). A role for *mel-18*, a Polycomb group-related vertebrate gene, during the anteroposterior specification of the axial skeleton. *Development* **122**, 1513-1522.
Akasaka, T., van Lohuizen, M., van der Lugt, N., Mizutani-Koseki, Y., Kanno, M., Taniguchi, M., Vidal, M., Alkema, M., Berns, A. and Koseki, H. (2001). Mice doubly deficient for the Polycomb Group genes *Mel18* and *Bmi1* reveal synergy and requirement for maintenance but not initiation of Hox gene expression. *Development* **128**, 1587-1597.
Alkema, M. J., Bronk, M., Verhoeven, E., Otte, A., van 't Veer, L. J., Berns, A. and van Lohuizen, M. (1997a). Identification of Bmi1-interacting proteins as constituents of a multimeric mammalian Polycomb complex. *Genes Dev.* **11**, 226-240.
Alkema, M. J., Jacobs, J., Voncken, J. W., Jenkins, N. A., Copeland, N. G., Satijn, D. P., Otte, A. P., Berns, A. and van Lohuizen, M. (1997b). MPc2, a new murine homolog of the *Drosophila* Polycomb protein is a member of the mouse Polycomb transcriptional repressor complex. *J. Mol. Biol.* **273**, 993-1003.
Atchison, L., Ghias, A., Wilkinson, F., Bonini, N. and Atchison, M. L. (2003). Transcription factor YY1 functions as a PcG protein in vivo. *EMBO J.* **22**, 1347-1358.
Bajusz, I., Sipos, L., Gyorgypal, Z., Carrington, E. A., Jones, R. S., Gausz, J. and Gyurkovics, H. (2001). The *Trithorax-mimic* allele of *Enhancer of zeste* renders active domains of target genes accessible to *Polycomb*-group-dependent silencing in *Drosophila melanogaster*. *Genetics* **159**, 1135-1150.
Barna, M., Merghoub, T., Costoya, J. A., Ruggero, D., Branford, M., Bergia, A., Samori, B. and Pandolfi, P. P. (2002). Plzf mediates transcriptional repression of *HoxD* gene expression through chromatin remodeling. *Dev. Cell* **3**, 499-510.
Bel, S., Coré, N., Djabali, M., Kieboom, K., van der Lugt, N., Alkema, M. J. and van Lohuizen, M. (1998). Genetic interactions and dosage effects of Polycomb group genes in mice. *Development* **125**, 3543-3551.

Bernstein, B. E., Kamal, M., Lindblad-Toh, K., Bekiranov, S., Bailey, D. K., Huebert, D. J., McMahon, S., Karlsson, E. K., Kulbokas, E. J. R., Gingeras, T. R. et al. (2005). Genomic maps and comparative analysis of histone modifications in human and mouse. *Cell* **120**, 169-181.

Bernstein, E., Duncan, E. M., Masui, O., Gil, J., Heard, E. and Allis, C. D. (2006). Mouse Polycomb proteins bind differentially to methylated histone H3 and RNA and are enriched in facultative heterochromatin. *Mol. Cell. Biol.* **26**, 2560-2569.

Boyer, L. A., Plath, K., Zeitlinger, J., Brambrink, T., Medeiros, L. A., Lee, T. I., Levine, S. S., Wernig, M., Tajonar, A., Ray, M. K. et al. (2006). Polycomb complexes repress developmental regulators in murine embryonic stem cells. *Nature* **441**, 349-353.

Bracken, A. P., Dietrich, N., Pasini, D., Hansen, K. H. and Helin, K. (2006). Genome-wide mapping of Polycomb target genes unravels their roles in cell fate transitions. *Genes Dev.* **20**, 1123-1136.

Breiling, A., Turner, B. M., Bianchi, M. E. and Orlando, V. (2001). General transcription factors bind promoters repressed by Polycomb group proteins. *Nature* **412**, 651-655.

Brown, J. L., Mucci, D., Whiteley, M., Dirksen, M. L. and Kassis, J. A. (1998). The *Drosophila* Polycomb group gene *pleiohomeotic* encodes a DNA binding protein with homology to the transcription factor YY1. *Mol. Cell* **1**, 1057-1064.

Campbell, R. B., Sinclair, D. A., Couling, M. and Brock, H. W. (1995). Genetic interactions and dosage effects of *Polycomb* group genes of *Drosophila*. *Mol. Gen. Genet.* **246**, 291-300.

Cao, R., Wang, L., Wang, H., Xia, L., Erdjument-Bromage, H., Tempst, P., Jones, R. S. and Zhang, Y. (2002). Role of histone H3 lysine 27 methylation in Polycomb-group silencing. *Science* **298**, 1039-1043.

Cao, R., Tsukada, Y. and Zhang, Y. (2005). Role of Bmi-1 and Ring1A in H2A ubiquitylation and Hox gene silencing. *Mol. Cell* **22**, 845-854.

Cheng, N. N., Sinclair, D. A., Campbell, R. B. and Brock, H. W. (1994). Interactions of *polyhomeotic* with *Polycomb* group genes of *Drosophila melanogaster*. *Genetics* **138**, 1151-1162.

Colberg-Poley, A. M., Voss, S. D., Chowdhury, K., Stewart, C. L., Wagner, E. F. and Gruss, P. (1985). Clustered homeo boxes are differentially expressed during murine development. *Cell* **43**, 39-45.

Coré, N., Bel, S., Gaunt, S. J., Aurrand-Lions, M., Pearce, J., Fisher, A. and Djabali, M. (1997). Altered cellular proliferation and mesoderm patterning in Polycomb-M33-deficient mice. *Development* **124**, 721-729.

Czermin, B., Melfi, R., McCabe, D., Seitz, V., Imhof, A. and Pirrotta, V. (2002). *Drosophila* enhancer of Zeste/ESC complexes have a histone H3 methyltransferase activity that marks chromosomal Polycomb sites. *Cell* **111**, 185-196.

de Napoles, M., Mermoud, J. E., Wakao, R., Tang, Y. A., Endoh, M., Appanah, R., Nesterova, T. B., Silva, J., Otte, A. P., Vidal, M. et al. (2004). Polycomb group proteins Ring1A/B link ubiquitylation of histone H2A to heritable gene silencing and X inactivation. *Dev. Cell* **7**, 663-676.

del Mar Lorente, M., Marcos-Gutierrez, C., Perez, C., Schoorlemmer, J., Ramirez, A., Magin, T. and Vidal, M. (2000). Loss- and gain-of-function mutations show a Polycomb group function for Ring1A in mice. *Development* **127**, 5093-5100.

Denisenko, O. N. and Bomsztyk, K. (1997). The product of the murine homolog of the *Drosophila extra sex combs* gene displays transcriptional repressor activity. *Mol. Cell. Biol.* **17**, 4707-4717.

Denisenko, O., Shnyreva, M., Suzuki, H. and Bomsztyk, K. (1998). Point mutations in the WD40 domain of Eed block its interaction with Ezh2. *Mol. Cell. Biol.* **18**, 5634-5642.

Deschamps, J., van den Akker, E., Forlani, S., De Graaff, W., Oosterveen, T., Roelen, B. and Roelfsema, J. (1999). Initiation, establishment and maintenance of *Hox* gene expression patterns in the mouse. *Int. J. Dev. Biol.* **43**, 635-650.

Dressler, G. R. and Gruss, P. (1989). Anterior boundaries of *Hox* gene expression in mesoderm-derived structures correlate with the linear gene order along the chromosome. *Differentiation* **41**, 193-201.

Eid, R., Koseki, H. and Schughart, K. (1993). Analysis of *LacZ* reporter genes in transgenic embryos suggests the presence of several *cis*-acting regulatory elements in the murine *Hoxb-6* gene. *Dev. Dyn.* **196**, 205-216.

Faust, C., Schumacher, A. and Magnuson, T. (1995). The *eed* mutation disrupts anterior mesoderm production in mouse. *Development* **121**, 273-285.

Faust, C., Lawson, K. A., Schork, N. J., Thiel, B. and Magnuson, T. (1998). The *Polycomb*-group gene *eed* is required for normal morphogenetic movements during gastrulation in the mouse embryo. *Development* **125**, 4495-4506.

Francis, N. J. and Kingston, R. E. (2001). Mechanisms of transcriptional memory. *Nat. Rev. Mol. Cell Biol.* **2**, 409-421.

Fritsch, C., Brown, J. L., Kassis, J. A. and Muller, J. (1999). The DNA-binding Polycomb group protein pleiohomeotic mediates silencing of a *Drosophila* homeotic gene. *Development* **126**, 3905-3913.

Fujimura, Y., Isono, K., Vidal, M., Endoh, M., Kajita, H., Mizutani-Koseki, Y., Takihara, Y., van Lohuizen, M., Otte, A., Jenuwein, T. et al. (2006). Distinct roles of Polycomb group gene products in transcriptionally repressed and active domains of *Hoxb8*. *Development* **133**, 2371-2381.

García, E., Marcos-Gutierrez, C., del Mar Lorente, M., Moreno, J. C. and Vidal, M. (1999). RYBP, a new repressor protein that interacts with components of the mammalian Polycomb complex, and with the transcription factor YY1. *EMBO J.* **18**, 3404-3418.

Gaunt, S. J. (1988). Mouse homeobox gene transcripts occupy different but overlapping domains in embryonic germ layers and organs: a comparison of *Hox-3.1* and *Hox-1.5*. *Development* **103**, 135-144.

Gaunt, S. J., Krumlauf, R. and Duboule, D. (1989). Mouse homeo-genes within a subfamily, Hox-1.4, -2.6 and -5.1, display similar anteroposterior domains of expression in the embryo, but show stage- and tissue-dependent differences in their regulation. *Development* **107**, 131-141.

Gaunt, S. J., Coletta, P. L., Pravtcheva, D. and Sharpe, P. T. (1990). Mouse *Hox-3.4*: Homeobox sequence and embryonic expression patterns compared with other members of the *Hox* gene network. *Development* **109**, 329-339.

Gilthorpe, J., Vandromme, M., Brend, T., Gutman, A., Summerbell, D., Totty, N. and Rigby, P. W. (2002). Spatially specific expression of *Hoxb4* is dependent on the ubiquitous transcription factor NFY. *Development* **129**, 3887-3899.

Gordon, S., Akopyan, G., Garban, H. and Bonavida, B. (2006). Transcription factor YY1: structure, function, and therapeutic implications in cancer biology. *Oncogene* **25**, 1125-1142.

Gould, A., Morrison, A., Sproat, G., White, R. A. and Krumlauf, R. (1997). Positive cross-regulation and enhancer sharing: two mechanisms for specifying overlapping *Hox* expression patterns. *Genes Dev.* **11**, 900-913.

Gunster, M. J., Satijn, D. P., Hamer, K. M., den Blaauwen, J. L., de Bruijn, D., Alkema, M. J., van Lohuizen, M., van Driel, R. and Otte, A. P. (1997). Identification and characterization of interactions between the vertebrate Polycomb-group protein BMI1 and human homologs of polyhomeotic. *Mol. Cell. Biol.* **17**, 2326-2335.

Hashimoto, N., Brock, H. W., Nomura, M., Kyba, M., Hodgson, J., Fujita, Y., Takihara, Y., Shimada, K. and Higashinakagawa, T. (1998). RAE28, BMI1, and M33 are members of heterogeneous multimeric mammalian Polycomb group complexes. *Biochem. Biophys. Res. Commun.* **245**, 356-365.

Hemenway, C. S., Halligan, B. W. and Levy, L. S. (1998). The Bmi-1 oncoprotein interacts with dinG and MPh2: the role of RING finger domains. *Oncogene* **16**, 2541-2547.

Hernandez-Munoz, I., Taghavi, P., Kuijl, C., Neefjes, J. and van Lohuizen, M. (2005). Association of BMI1 with Polycomb bodies is dynamic and requires PRC2/EZH2 and the maintenance DNA methyltransferase DNMT1. *Mol. Cell. Biol.* **25**, 11047-11058.

Isono, K., Fujimura, Y., Shinga, J., Yamaki, M., O-Wang, J., Takihara, Y., Murahashi, Y., Takada, Y., Mizutani-Koseki, Y. and Koseki, H. (2005). Mammalian Polyhomeotic homologues Phc2 and Phc1 act in synergy to mediate Polycomb repression of *Hox* genes. *Mol. Cell. Biol.* **25**, 6694-6706.

Jin, Q., van Eynde, A., Beullens, M., Roy, N., Thiel, G., Stalmans, W. and Bollen, M. (2003). The Protein Phosphatase-1 (PP1) regulator, Nuclear Inhibitor of PP1 (NIPP1), interacts with the Polycomb group protein, Embryonic Ectoderm Development (EED), and functions as a transcriptional repressor. *J. Biol. Chem.* **278**, 30677-30685.

Jürgens, G. (1985). A group of genes controlling the spatial expression of the bithorax complex in *Drosophila*. *Nature* **316**, 153-155.

Kalantry, S. and Magnuson, T. (2006). The Polycomb group protein EED is dispensable for the initiation of random X-chromosome inactivation. *PLoS Genet.* **2**, 656-664.

Kalantry, S., Mills, K. C., Yee, D., Otte, A. P., Panning, B. and Magnuson, T. (2006). The Polycomb group protein Eed protects the inactive X-chromosome from differentiation-induced reactivation. *Nat. Cell Biol.* **8**, 195-202.

Katoh-Fukui, Y., Tsuchiya, R., Shiroishi, T., Nakahara, Y., Hashimoto, N., Noguchi, K. and Higashinakagawa, T. (1998). Male-to-female sex reversal in *M33* mutant mice. *Nature* **393**, 688-692.

Kennison, J. A. and Tamkun, J. W. (1988). Dosage-dependent modifiers of Polycomb and Antennapedia mutations in *Drosophila*. *Proc. Natl. Acad. Sci. USA* **85**, 8136-8140.

Kessel, M. and Gruss, P. (1991). Homeotic transformations of murine vertebrae and concomitant alterations of *Hox* codes induced by retinoic acid. *Cell* **67**, 89-104.

Kuzmichev, A., Nishioka, K., Erdjument-Bromage, H., Tempst, P. and Reinberg, D. (2002). Histone methyltransferase activity associated with a human multiprotein complex containing the Enhancer of Zeste protein. *Genes Dev.* **16**, 2893-2905.

Kuzmichev, A., Jenuwein, T., Tempst, P. and D. R. (2004). Different EZH2-containing complexes target methylation of histone H1 or nucleosomal histone H3. *Mol. Cell* **14**, 183-193.

Kuzmichev, A., Margueron, R., Vaquero, A., Preissner, T. S., Scher, M., Kirmizis, A., Ouyang, X., Brockdorff, N., Abate-Shen, C., Farnham, P. et al. (2005). Composition and histone substrates of Polycomb repressive group complexes change during cellular differentiation. *Proc. Natl. Acad. Sci. USA* **102**, 1859-1864.

Lee, T. I., Jenner, R. G., Boyer, L. A., Guenther, M. G., Levine, S. S., Kumar, R. M., Chevalier, B., Johnstone, S. E., Cole, M. F., Isono, K. et al. (2006).

Control of developmental regulators by Polycomb in human embryonic stem cells. *Cell* **125**, 301-313.
Lessard, J., Schumacher, A., Thorsteinsdottir, U., van Lohuizen, M., Magnuson, T. and Sauvageau, G. (1999). Functional antagonism of the *Polycomb*-Group genes *eed* and *Bmi1* in hemopoietic cell proliferation. *Genes Dev.* **13**, 2691-2703.
Levine, S. S., Weiss, A., Erdjument-Bromage, H., Shao, Z., Tempst, P. and Kingston, R. E. (2002). The core of the Polycomb repressive complex is compositionally and functionally conserved in flies and humans. *Mol. Cell. Biol.* **22**, 6070-6078.
Lorente, M., Perez, C., Sanchez, C., Donohoe, M., Shi, Y. and Vidal, M. (2006). Homeotic transformations of the axial skeleton of *YY1* mutant mice and genetic interaction with the Polycomb group gene *Ring1/Ring1A*. *Mech. Dev.* **123**, 312-320.
Lund, A. H. and van Lohuizen, M. (2004). Polycomb complexes and silencing mechanisms. *Curr. Opin. Cell Biol.* **16**, 239-246.
Mager, J., Montgomery, N. D., de Villena, F. P. and Magnuson, T. (2003). Genome imprinting regulated by the mouse Polycomb group protein Eed. *Nat. Genet.* **33**, 502-507.
Mak, W., Baxter, J., Silva, J., Newall, A. E., Otte, A. P. and Brockdorff, N. (2002). Mitotically stable association of Polycomb group proteins Eed and Enx1 with the inactive X chromosome in trophoblast stem cells. *Curr. Biol.* **12**, 1016-1020.
Mann, R. S. (1997). Why are *Hox* genes clustered? *BioEssays* **19**, 661-664.
Mihaly, J., Mishra, R. K. and Karch, F. (1998). A conserved sequence motif in *Polycomb*-response elements. *Mol. Cell* **1**, 1065-1066.
Mok, H., Jelinek, J., Pai, S., Cattanach, B. M., Prchal, J. T., Youssoufian, H. and Schumacher, A. (2004). Disruption of ferroportin 1 regulation causes dynamic alterations in iron homeostasis and erythropoiesis in polycythaemia mice. *Development* **131**, 1859-1868.
Mok, H., Mlodnicka, A. E., Hentze, M. W., Muckenthaler, M. and Schumacher, A. (2006). The molecular circuitry regulating the switch between iron deficiency and overload in mice. *J. Biol. Chem.* **281**, 7946-7951.
Montgomery, N. D., Yee, D., Chen, A., Kalantry, S., Chamberlain, S. J., Otte, A. P. and Magnuson, T. (2005). The murine Polycomb group protein Eed is required for global histone H3 lysine-27 methylation. *Curr. Biol.* **15**, 942-947.
Müller, J., Hart, C. M., Francis, N. J., Vargas, M. L., Sengupta, A., Wild, B., Miller, E. L., O'Connor, M. B., Kingston, R. E. and Simon, J. A. (2002). Histone methyltransferase activity of a *Drosophila* Polycomb group repressor complex. *Cell* **111**, 197-208.
Neubüser, A., Koseki, H. and Balling, R. (1995). Characterization and developmental expression of *Pax9*, a paired-box-containing gene related to *Pax1*. *Dev. Biol.* **170**, 701-716.
Ng, J., Li, R., Morgan, K. and Simon, J. (1997). Evolutionary conservation and predicted structure of the *Drosophila* extra sex combs repressor protein. *Mol. Cell. Biol.* **17**, 6663-6672.
Otte, A. P. and Kwaks, T. H. J. (2003). Gene repression by Polycomb group protein complexes: a distinct complex for every occasion? *Curr. Opin. Genet. Dev.* **13**, 448-454.
Paro, R. and Hogness, D. S. (1991). The Polycomb protein shares a homologous domain with a heterochromatin-associated protein of *Drosophila*. *Proc. Natl. Acad. Sci. USA* **88**, 263-267.
Peytavi, R., Hong, S. S., Gay, B., d'Angeac, A. D., Selig, L., Benichou, S., Benarous, R. and Boulanger, P. (1999). HEED, the product of the human homolog of the murine *eed* gene, binds to the matrix protein of HIV-1. *J. Biol. Chem.* **274**, 1635-1645.
Pirrotta, V., Poux, S., Melfi, R. and Pilyugin, M. (2003). Assembly of Polycomb complexes and silencing mechanisms. *Genetica* **117**, 191-197.
Plath, K., Fang, J., Mlynarczyk-Evans, S. K., Cao, R., Worringer, K. A., Wang, H., de la Cruz, C. C., Otte, A. P., Panning, B. and Zhang, Y. (2003). Role of histone H3 lysine 27 methylation in X inactivation. *Science* **300**, 131-135.
Poux, S., Melfi, R. and Pirrotta, V. (2001). Establishment of Polycomb silencing requires a transient interaction between PC and ESC. *Genes Dev.* **15**, 2509-2514.
Ramirez-Solis, R., Zheng, H., Whiting, J., Krumlauf, R. and Bradley, A. (1993). *Hoxb-4* (*Hox-2.6*) mutant mice show homeotic transformation of a cervical vertebra and defects in the closure of the sternal rudiments. *Cell* **73**, 279-294.
Richie, E. R., Schumacher, A., Angel, J. M., Holloway, M., Rinchik, E. M. and Magnuson, T. (2002). The *Polycomb*-group gene *eed* regulates thymocyte differentiation and suppresses the development of carcinogen-induced T-cell lymphomas. *Oncogene* **21**, 299-306.
Rietzler, M., Bittner, M., Kolanus, W., Schuster, A. and Holzmann, B. (1998). The human WD repeat protein WAIT-1 specifically interacts with the cytoplasmic tails of β7-integrins. *J. Biol. Chem.* **273**, 27459-27466.
Rinchik, E. M. and Carpenter, D. A. (1999). *N*-ethyl-*N*-nitrosourea mutagenesis of a 6- to 11-cM subregion of the *Fah-Hbb* interval of mouse chromosome 7: Completed testing of 4557 gametes and deletion mapping and complementation analysis of 31 mutations. *Genetics* **152**, 373-383.
Ringrose, L. and Paro, R. (2004). Epigenetic regulation of cellular memory by the Polycomb and Trithorax group proteins. *Annu. Rev. Genet.* **38**, 413-443.
Sanchez-Elsner, T., Gou, D., Kremmer, E. and Sauer, F. (2006). Noncoding RNAs of trithorax response elements recruit *Drosophila* Ash1 to Ultrabithorax. *Science* **311**, 1118-1123.
Satijn, D. P. and Otte, A. P. (1999). RING1 interacts with multiple Polycomb-group proteins and displays tumorigenic activity. *Mol. Cell. Biol.* **19**, 57-68.
Satijn, D. P., Gunster, M. J., van der Vlag, J., Hamer, K. M., Schul, W., Alkema, M. J., Saurin, A. J., Freemont, P. S., van Driel, R. and Otte, A. P. (1997). RING1 is associated with the Polycomb group protein complex and acts as a transcriptional repressor. *Mol. Cell. Biol.* **17**, 4105-4113.
Satijn, D. P., Hamer, K. M., den Blaauwen, J. and Otte, A. P. (2001). The Polycomb group protein EED interacts with YY1, and both proteins induce neural tissue in *Xenopus* embryos. *Mol. Cell. Biol.* **21**, 1360-1369.
Saurin, A. J., Shao, Z., Erdjument-Bromage, H., Tempst, P. and Kingston, R. E. (2001). A *Drosophila* Polycomb group complex includes Zeste and dTAFII proteins. *Nature* **412**, 655-660.
Schoorlemmer, J., Marcos-Gutierrez, C., Were, F., Martinez, R., Garcia, E., Satijn, D. P., Otte, A. P. and Vidal, M. (1997). Ring1A is a transcriptional repressor that interacts with the Polycomb-M33 protein and is expressed at rhombomere boundaries in the mouse hindbrain. *EMBO J.* **16**, 5930-5942.
Schughart, K., Utset, M. F., Awgulewitsch, A. and Ruddle, F. H. (1988). Structure and expression of Hox-2.2, a murine homeobox-containing gene. *Proc. Natl. Acad. Sci. USA* **85**, 5582-5586.
Schumacher, A., Faust, C. and Magnuson, T. (1996). Positional cloning of a global regulator of anterior-posterior patterning in mice. *Nature* **383**, 250-253.
Schumacher, A., Lichtarge, O., Schwartz, S. and Magnuson, T. (1998). The murine *Polycomb*-group gene *eed* and its human orthologue: functional implications of evolutionary conservation. *Genomics* **54**, 79-88.
Schwartz, Y. B., Kahn, T. G., Nix, D. A., Li, X. Y., Bourgon, R., Biggin, M. and Pirrotta, V. (2006). Genome-wide analysis of Polycomb targets in *Drosophila melanogaster*. *Nat. Genet.* **38**, 700-705.
Sewalt, R. G. A. B., van der Vlag, J., Gunster, M. J., Hamer, K. M., den Blaauwen, J. L., Satijn, D. P. E., Hendrix, T., van Driel, R. and Otte, A. P. (1998). Characterization of interactions between the mammalian Polycomb-group proteins Enx1/EZH2 and EED suggests the existence of different mammalian Polycomb-group protein complexes. *Mol. Cell. Biol.* **18**, 3586-3595.
Sham, M. H., Hunt, P., Nonchev, S., Papalopulu, N., Graham, A., Boncinelli, E. and Krumlauf, R. (1992). Analysis of the murine *Hox-2.7* gene: conserved alternative transcripts with differential distributions in the nervous system and the potential for shared regulatory regions. *EMBO J.* **11**, 1825-1836.
Shao, Z., Raible, F., Mollaaghababa, R., Guyon, J. R., Wu, C. T., Bender, W. and Kingston, R. E. (1999). Stabilization of chromatin structure by PRC1, a Polycomb complex. *Cell* **98**, 37-46.
Shrivastava, A. and Calame, K. (1994). An analysis of genes regulated by the multi-functional transcriptional regulator Yin Yang-1. *Nucleic Acids Res.* **22**, 5151-5155.
Silva, J., Mak, W., Zvetkova, I., Appanah, R., Nesterova, T. B., Webster, Z., Peters, A. H., Jenuwein, T., Otte, A. P. and Brockdorff, N. (2003). Establishment of histone h3 methylation on the inactive X chromosome requires transient recruitment of Eed-Enx1 Polycomb group complexes. *Dev. Cell* **4**, 481-495.
Suzuki, M., Mizutani-Koseki, Y., Fujimura, Y., Miyagishima, H., Kaneko, T., Takada, Y., Akasaka, T., Tanzawa, H., Takihara, Y., Nakano, M. et al. (2002). Involvement of the Polycomb-group gene *Ring1B* in the specification of the anterior-posterior axis in mice. *Development* **129**, 4171-4183.
Takihara, Y., Tomotsune, D., Shirai, M., Katoh-Fukui, Y., Nishii, K., Motaleb, M. A., Nomura, M., Tsuchiya, R., Fujita, Y., Shibata, Y. et al. (1997). Targeted disruption of the mouse homologue of the *Drosophila polyhomeotic* gene leads to altered anteroposterior patterning and neural crest defects. *Development* **124**, 3673-3682.
Tolhuis, B., Muijrers, I., de Wit, E., Teunissen, H., Talhout, W., van Steensel, B. and van Lohuizen, M. (2006). Genome-wide profiling of PRC1 and PRC2 Polycomb chromatin binding in *Drosophila melanogaster*. *Nat. Genet.* **38**, 694-699.
Tomotsune, D., Shirai, M., Takihara, Y. and Shimada, K. (2000). Regulation of *Hoxb3* expression in the hindbrain and pharyngeal arches by *rae28*, a member of the mammalian *Polycomb* group of genes. *Mech. Dev.* **98**, 165-169.
van der Lugt, N. M. T., Domen, J., Linders, K., van Roon, M., Robanus-Maandag, E., Riele, H., van der Valk, M., Deschamps, J., Sofroniew, M., van Lohuizen, M. et al. (1994). Posterior transformation, neurological abnormalities, and severe hematopoietic defects in mice with targeted deletion of the *bmi-1* proto-oncogene. *Genes Dev.* **8**, 757-769.
van der Lugt, N. M. T., Alkema, M., Berns, A. and Deschamps, J. (1996). The *Polycomb*-group homolog Bmi-1 is a regulator of murine *Hox* gene expression. *Mech. Dev.* **58**, 153-164.
van der Vlag, J. and Otte, A. P. (1999). Transcriptional repression mediated by the human Polycomb-group protein EED involves histone deacetylation. *Nat. Genet.* **23**, 474-478.
van Lohuizen, M., Tijms, M., Voncken, J. W., Schumacher, A., Magnuson, T.

and Wientjens, E. (1998). Interaction of mouse Polycomb-group (Pc-G) proteins Enx1 and Enx2 with Eed: indication for separate Pc-G complexes. *Mol. Cell. Biol.* **18**, 3572-3579.
Verbout, A. J. (1985). The development of the vertebral column. *Adv. Anat. Embryol. Cell Biol.* **90**, 1-122.
Voncken, J. W., Roelen, B. A., Roefs, M., de Vries, S., Verhoeven, E., Marino, S., Deschamps, J. and van Lohuizen, M. (2003). *Rnf2* (*Ring1b*) deficiency causes gastrulation arrest and cell cycle inhibition. *Proc. Natl. Acad. Sci. USA* **100**, 2468-2473.
Wang, H., Wang, L., Erdjument-Bromage, H., Vidal, M., Tempst, P., Jones, R. S. and Zhang, Y. (2004). Role of histone H2A ubiquitination in Polycomb silencing. *Nature* **431**, 873-878.
Wang, J., Mager, J., Chen, Y., Schneider, E., Cross, J. C., Nagy, A. and Magnuson, T. (2001). Imprinted X inactivation maintained by a mouse *Polycomb* group gene. *Nat. Genet.* **28**, 371-375.
Wang, J., Mager, J., Schneider, E. and Magnuson, T. (2002). The mouse *PcG* gene *eed* is required for *Hox* gene repression and extraembryonic development. *Mamm. Genome* **13**, 493-503.
Wang, L., Brown, J. L., Cao, R., Zhang, Y., Kassis, J. A. and Jones, R. S. (2004). Hierarchical recruitment of Polycomb group silencing complexes. *Mol. Cell* **14**, 637-646.
Wilkinson, D. G. and Nieto, M. A. (1993). Detection of messenger RNA by *in situ* hybridization to tissue sections and whole mounts. In *Guide to Techniques in Mouse Development (Methods in Enzymology)*. Vol. 225 (ed. P. M. Wassarman and M. L. DePamphilis), pp. 361-373. San Diego: Academic Press.
Yu, B. D., Hess, J. L., Horning, S. E., Brown, G. A. J. and Korsmeyer, S. J. (1995). Altered *Hox* expression and segmental identity in *Mll*-mutant mice. *Nature* **378**, 505-508.
Yu, B. D., Hanson, R. D., Hess, J. L., Horning, S. E. and Korsmeyer, S. J. (1998). MLL, a mammalian *trithorax*-group gene, functions as a transcriptional maintenance factor in morphogenesis. *Proc. Natl. Acad. Sci. USA* **95**, 10632-10636.